International Conference on Applied Energy 2020
Dec. 1 - Dec. 10, 2020, Bangkok / Virtual
Paper ID: 513

Impact of winding angle on falling film thickness in spiral wound heat exchangers

Na He [1, 3] , Xuedong Chen [2] , Yongdong Chen [2*], Shurong Yu[1], Xiaohong Wu [2] , Xue Li [2]

1 College of Petrochemical Engineering, Lanzhou University of Technology, Lanzhou 730050, Gansu, China

2 Hefei General Machinery Research Institute Limited Company, Hefei 230031, Anhui, China

3 Bailie College of Petroleum Engineering, Lanzhou City University , Lanzhou 730070, Gansu, China

ABSTRACT

A three-dimensional model is applied in this paper to simulate the falling film flow on shell-side of the spiral wound heat exchangers (SWHEs), the flow behavior is simulated with winding angle varied from 0° to 20°. The falling film process of the spiral tube is analyzed and film thickness is measured in axial and circumferential direction. Meanwhile the dimensionless parameter of maldistribution is defined to evaluate the thickness distribution deviating from the ideal condition and the maldistribution is calculated with the simulated results. Results show that the winding angle can influence the flow behavior. The maximum film thickness decreases with the increase of the winding angle at the same circumferential angle. The ascending flow region reduces and the declining flow region enlarges with the winding angle increasing. The maldistribution declines with the winding angle increasing.

Keywords: spiral wound heat exchangers, film thickness, maldistribution, numerical simulation

NONMENCLATURE

Symbols	
E	the maldistribution
g	gravitational acceleration, m/s^2
l	distance from the measuring point to liquid column, mm
l*	dimensionless length
L	spray hole spacing, mm
m	the quantity of measuring points along the axial direction
n	the quantity of measuring points along the circumferential direction
Re	Reynolds number
t	time, s
v	fluid velocity, m/s
x, y, z	Cartesian coordinates direction
Greek	
β	winding angle, °
δ	film thickness, mm
Θ	circumferential angle, °
μ	dynamic viscosity, pa·s
ρ	density, kg/m^3
σ	surface tension, N/m
Subscripts	
Θ	circumferential angle
x, y, z	Cartesian coordinates direction

1. INTRODUCTION

Spiral wound heat exchangers (SWHEs) are widely used in the refrigeration, food industry, petroleum and chemical due to the characteristic of higher heat transfer efficiency, compact structure, multi-stream heat exchange and chosen as the main cryogenic heat exchanger by the most base load LNG plants. In spiral wound exchangers, the refrigerant evaporates on the

Selection and peer-review under responsibility of the scientific committee of the 12th Int. Conf. on Applied Energy (ICAE2020).

shell-side in form of falling film flow and the streams condense on the tube-side in form of upward flow [1-2]. For falling film evaporation process, the flow pattern of fluid effect on heat transfer performance of heat exchanger. The thickness of falling film is one of the most important parameters that influenced the heat transfer resistance and the performance of heat and mass transfer. Moreover, the thickness of falling film is related to the stability of the falling flow, which is critical for the whole falling film evaporation process [3].

The researches on falling films have been conducted by both theoretical and practical approaches in the past years. Nusselt[4] first analyzed falling films theoretically, assuming a continuous sheet flow between the tube and the effects of momentum on the falling films was negligible, a classical method of the film thickness was proposed. Zhang et al. [5] measured the film thickness of a horizontal corrugated tube by the conductance probe methods, the corrugated radius varying from 0.25 to 1 mm and a new correlation was given to predict the film thickness of the corrugated tube. Hou et al. [6] investigated the thickness distribution of the horizontal tube and a new correlation was presented to predict the film thickness based on the experimental data. Arjun Jayakumar et al. [7] developed a non-intrusive technique to measure film thickness of the horizontal tube with Re ranging from 130 to 350. Anders Åkesjö et al.[8] adopted two measurement procedures to expound the features of vertical falling films, the film thickness was measured continuously along a 0.10 m long vertical line.

With the development of computational fluid dynamics, some scholars have studied the falling film thickness by numerical simulation. Han et al. [9] developed a 3-D simulation to analyze the fluid characteristic of curved egg-shaped tube, the axial and circumferential distribution of film thickness was measured with Re varying from 327 to 2944. Tahira et al. [10] performed a 2-D model to research the effects of viscosity and surface tension, the film thickness was calculated with different surface tension and viscosity. Qiu et al. [11] adopted a 3-D model to simulate the falling film process with Re varied from 171 to 368, the maximum elongation distance of the liquid film was measured. Wang et al. [12] employed a three-dimensional numerical simulation to investigate falling film of the horizontal tube with column flow. The film thickness distribution along circumferential and axial direction was calculated with the tube spacing ranging from 10 to 30 mm and Re varying from 221 to 295.

The falling film flow around the tube included the horizontal tube falling film flow and vertical tube falling film flow. The research of falling film flow focused on the variation of film thickness influenced by tube shape, Re and physical properties. Due to the heat transfer coefficient of horizontal tube falling film evaporation is about twice as much as that of the vertical tube evaporation, most of the falling film research was concentrated on the horizontal tube falling film flow. The winding angle of SWHEs is varied from 5° to 20° in general, it is relatively small and similar with horizontal tube falling film evaporation. In order to analyse the influence with the spiral angle and compare the results with the horizontal tube, the winding angle at 0°, 5°, 10°, 15°, 20° are adopted to simulate the falling film flow around the tube, numerical model employed the 3-D model to capture the film thickness along the axial and circumferential directions.

2. NUMERICAL APPROACH

2.1 Physical model

The SWHEs consist of multiple coils wound helically around a center mandrel, the different tubes are coiled in layers around the central core, the coiling direction alternates from one layer to the next. The refrigerant flows downward in form of falling film on tube bundles of SWHEs. In this study, the propane was chosen as refrigerant at working temperature -25.4℃ and operating pressure 0.2MPa, the fluid physical properties is listed in Table 1.

Table 1

Physical properties of propane

Phase	ρ $Kg{\cdot}m^{-3}$	μ $Pa{\cdot}s$	σ $N{\cdot}m^{-1}$
liquid	561	1.64×10^{-4}	0.013
vapor	4.54	6.81×10^{-6}	/

2.2 Assumptions

For the simplification of the physical model, the following assumptions have been made:

1) The physical properties of liquid are constant.
2) The falling film is analyzed under adiabatic condition.
3) The shear force of the gas phase is not considered.
4) The spiral tube is straight in local, the bending of spiral tube is ignored.

2.3 Geometry model and boundary conditions

A 3-D model is established to analysis the falling film flow of the spiral tube, in order to save the computation time, the solution domain is considered as the symmetrical structure and the half of the flow area is chosen to calculate as shown in Fig 1. The diameter of the spiral tube is 12mm, the diameter of the spray holes is 2mm, the spray hole spacing is 10mm and the distribution height is 10mm. The liquid inlet is set to be velocity-inlet boundary with the volume fraction of propane in liquid equals 1.0. The rest of the top part of the model is set as velocity-inlet boundary with the volume fraction of propane in gas equals 1.0. The surface of tube wall is set to be wall boundary, the contact angle between the liquid and the wall is set to 10°. The x-direction boundaries are set as periodic boundary. The z-direction boundaries are set as symmetry boundary and the bottom is set as outflow boundary.

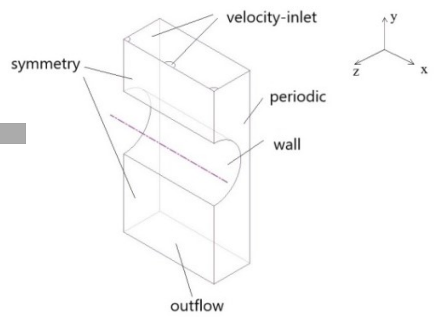

Fig 1 Three-dimension model

In order to simplify the model and be easy to measure the film thickness, the inclination of the spiral tube is realized by changing the gravitational acceleration vector and the velocity components of horizontal tube falling film flow, the transition from the tube inclination to the gravitational acceleration as shown in Fig 2.

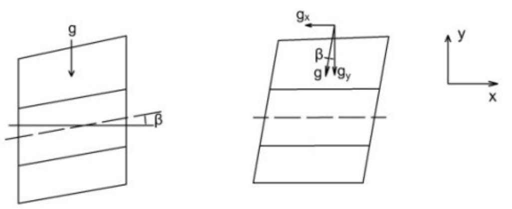

(a) Tube inclination (b) Gravitational fields inclination

Fig 2 Transition diagram

The gravitational acceleration is calculated as follow:

$$g_x = g \sin\beta \quad (1)$$

$$g_y = g \cos\beta \quad (2)$$

$$g_z = 0 \quad (3)$$

where B is the winding angle. In order to compare the model with the equally spray density and make sure the gravitational acceleration and the velocity in the same direction, the velocity components are calculated as follow:

$$v_x = v \sin\beta \quad (4)$$

$$v_y = v \cos\beta \quad (5)$$

$$v_z = 0 \quad (6)$$

2.4 Mathematical methods

In this study, the falling film flow is considered as a laminar flow according to Reynolds number. The Volume of Fluid (VOF) model is used to capture the gas-liquid interface, treating gas as the primary phase and liquid as the second phase. Considering the influence of the surface tension on the gas-liquid interface, the continuum surface force (CSF) model is adopted and. The Pressure-Implicit with Splitting of Operators (PISO) scheme is chosen for the pressure-velocity coupling. The second-order upwind scheme is utilized to deal with the pressure and momentum equation.

2.5 Grid independence and model validation

The computational domain is performed with unstructured grid, the grid is refined in the region around the tube wall to precisely capture the flow behavior of the falling film flow. Three numerical models with element number of 430368, 654624 and 958800 separately are taken into consideration. The film thicknesses of three typical circumferential angles θ=45°, θ=90° and θ=135° is traced, it found that the difference in film thickness between grid of 654624 elements and 958800 elements is below 5%, Therefore, a grid of 654624 cells with a minimum cell length of 0.08 mm and a maximum length of 0.25mm is adopted in the simulation.

In this study, the numerical approach is validated with the Chen et al. [13] study in the same working conditions, the results are shown in Fig 3. The numerical results are compared with the experimental data, the numerical result agrees well with the experimental data in the overall trend and the numerical results were less than the experimental data, the biggest difference between them is less than 20%. The reason for this could be the numerical model is limited by the size of the model resulted that the flux of the liquid column was less than the experimental data. Considering the instability of the falling film process and data comparison, the simulation results are reliable.

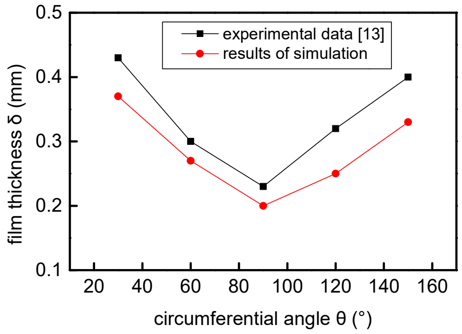

Fig 3 Validation of the numerical model

3. RESULTS AND DISCUSSION

3.1 The process of the falling film flow

Fig 4 describes the flow process when the Reynolds number is approximately 1073 at the winding angle is 10°. The falling film descends with its initial velocity (v=0.5m/s) by the effect of gravity and inertia force (Fig4(a)-(b)), then the liquid column impacts the top of tube wall, the impact makes fluid spread in different directions in the form of thin film, the axial flow and the circumferential flow are regarded as two main directions. In the axial flow, the liquid column spread with different fluid quantity on two sides of the fluid column influenced by the winding angel, the fluid quantity of ascending side is less than that of descent side, the two fluids from the adjacent columns cause overlap limited by the distance between the inlet column as shown in Fig 4(c), In the circumferential direction, the falling film spread on the tube wall in the direction of gravity (Fig 4(d)-(e)). The liquid film shrinks and gathers at the bottom of the tube, a new liquid

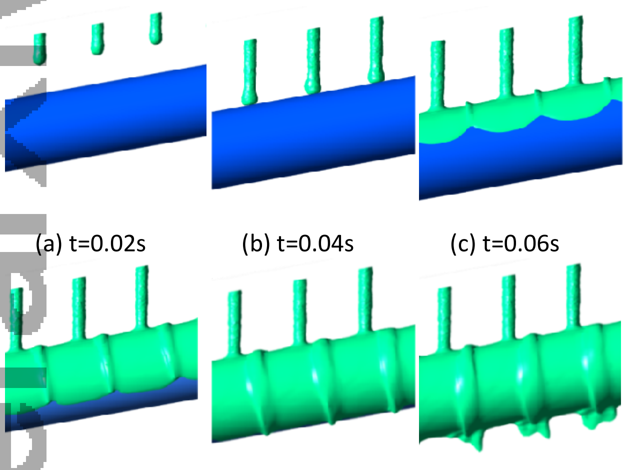
(a) t=0.02s (b) t=0.04s (c) t=0.06s

(d) t=0.08s (e) t=0.1s (f) t=0.12s

Fig 4 Process of falling film flow with Re=1073

column is formed with the fluid continuously accumulated and then flows to the next tubes (Fig 4(f)). The falling film shows periodic distribution between the two adjacent liquid columns.

3.2 The spatial distribution of falling film

In this study, one periodic length is concerned to analyze the film distribution, a dimensionless parameter l* is introduced to describe the variability of the film thickness along axial direction, it is defined as follow:

$$l^* = \frac{l}{L} \qquad (7)$$

Where L is the distance between the two center lines of the adjacent column with fixed value of 10mm, l is distance from the center line of the left liquid column to the measurement point. Fig 5 shows the variation of the film thickness is a function of the parameter l*, the distribution of the film thickness at different circumferential angle is shown in Fig 5 (a)-(d). In order to analysis the falling film feature at different winding angle, two special cross sections are proposed as shown in Fig 6, the section slide with the center of the fluid column is named as impingement cross section which is located at l* =0 (section a) or l* =1(section c), and the section slide with the maximum film thickness is named as crest cross section (section b). The falling film outside the spiral tube is divided into two regions: the region between the first impingement cross section (l* =0) and the crest cross section is defined as ascending flow section (from section a to section b) and the region between the crest cross section and the second impingement cross section (l* =1) is defined as the declining flow section (from section b to section c).

From Fig 5, it is found that the maximum film thickness decreases with the winding angle increasing at the same circumferential angle and the location of crest cross section is changed with the winding angle, the l* of crest cross section reduces with the spiral angle increasing, the crest cross section is located at l*=0.5 with β=0° and located at l*=0.3 with β=20°. The film thickness is symmetrical distribution along the two sides of the crest cross section at β=0°, the ascending flow region reduced and the declining flow region enlarged with the spiral angle increasing and the film thickness of the ascending flow section is larger than that of the declining flow section. That may be caused by falling film spreads along the axial direction which cause down flow increased with the winding angle ascent.

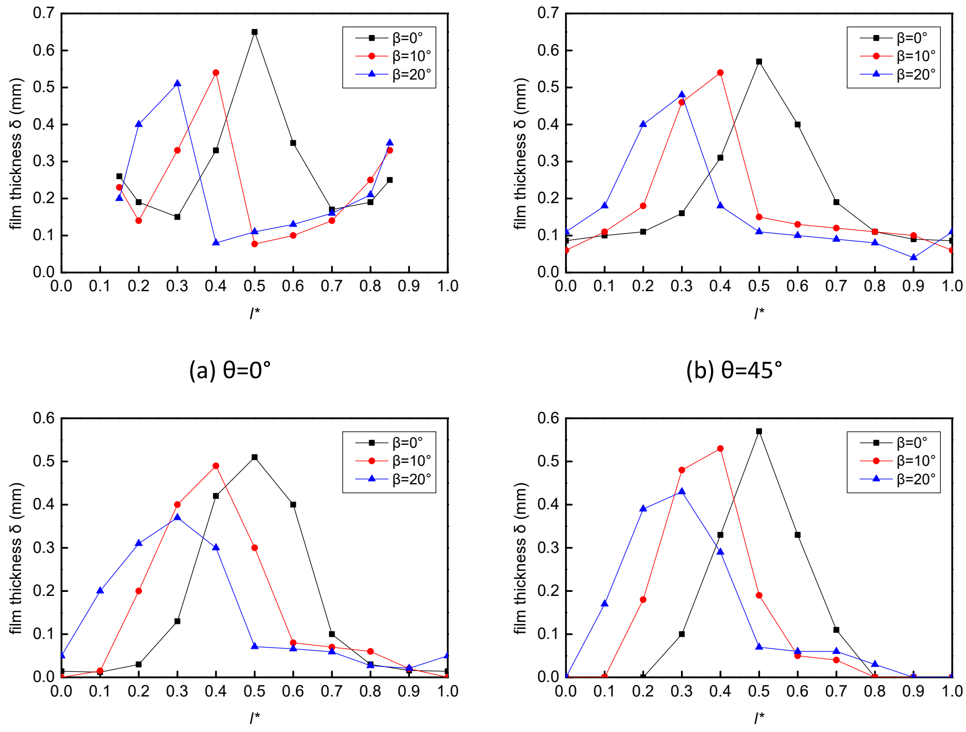

(a) θ=0°　　(b) θ=45°

(c) θ=90°　　(d) θ=135°

Fig 5 Distribution of film thickness

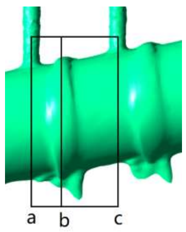

Fig 6 Partition of the falling film

3.3 The analysis of thickness maldistribution

From Fig 5, it is found that the thickness distribution is not uniform, some section is large and other section is small, even dryout section appear on the pipe surface, the main causes of this non-uniformity distribution lie in fluid film stressed differently at different positions on the pipe surface.

In the process of falling film evaporation, the distribution of liquid film outside the tube affects the heat transfer performance of the heat exchanger. The heat transfer resistance increases when the film thickness is too large, the liquid film thickness decreases to a certain extent, and there is a dryout section appear outside the tube, which will lead to the liquid cannot participate in the heat transfer, and the performance of the heat exchanger will be deteriorated. In the ideal conditions, there is a stable and uniform falling film outside the tube during falling film evaporation. However, in the actual falling film, the liquid film outside the tube is not uniform influenced by various factors, such as the evaporator structure, the operating conditions and fluid physical properties and so on. In order to evaluate the deviation degree of the film thickness distribution from the ideal state, the dimensionless parameter E is given to evaluate maldistribution of the liquid film distribution, E is calculated as follow:

$$E_{\theta} = \frac{1}{\mathrm{m}}\sum_{l^*=0}^{1}\frac{1}{\bar{\delta}_{\theta}}\left|\delta_{\theta l^*} - \bar{\delta}_{\theta}\right| \qquad (8)$$

$$E = \frac{1}{\mathrm{n}}\sum_{\theta=0}^{2\pi} E_{\theta} \qquad (9)$$

E_θ is maldistribution of the liquid film distribution along the axial direction when the circumferential angle is θ, m is the quantity of measuring points along the axial direction, n is the quantity of the measuring points along the circumference direction. $\bar{\delta}_\theta$ is the average film thickness when the circumferential angle is θ, in this paper the method of Nusselt[4] is adopted to calculate the $\bar{\delta}_\theta$, shown as follow:

$$\bar{\boldsymbol{\delta}}_{\boldsymbol{\theta}} = \left(\frac{3\mu\Gamma}{\rho^2 g \sin\theta}\right)^{\frac{1}{3}} \qquad (10)$$

E is calculated with the simulate results show in Fig 7, it is found that E_θ increases with the winding angle increasing at θ=0° and decreased with the winding angle increasing at θ=90°and θ=145°, there is no obvious rule at θ=45°. E decreases with the winding angle increasing.

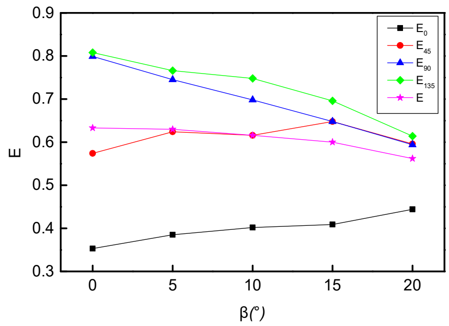

Fig 7 Maldistribution of the film thickness

4. CONCLUSIONS

A 3-D model is applied to investigate the spiral tube falling-film process with the winding angle at 0°, 5°, 10°, 15°, 20° and Re=1073. The film thickness is measured in both axial and circumferential directions. Moreover, the maldistribution E is defined to evaluate the distribution of the film thickness and calculated with the simulation results. The main conclusions are obtained as follows:

1) The ascending flow section decreases and the declining flow section increases with the winding angle increasing.
2) The film thickness of the crest cross section decreases with the winding angle increasing.
3) The maldistribution E_θ increases with the spiral angle increasing at θ=0° and decreases with the winding angle increasing at θ=90° and θ=145°, there is no obvious rule at θ=45°.
4) The maldistribution E decreases with the winding angle increasing.

ACKNOWLEDGEMENT

The present work is supported by the key R&D program of Anhui province (grant number 201904a05020050)

REFERENCE

[1] Neeraasa BO, Fredheim AO, Aunan B. Experimental data and model for heat transfer, in liquid falling film flow on shell-side, for spiral-wound LNG heat exchanger. J. International Journal of Heat and Mass Transfer 2004; 47: 3565–3572.

[2] Neeraasa BO, Fredheim AO, Aunan B. Experimental shell-side heat transfer and pressure drop in gas flow for spiral-wound LNG heat exchanger. J. International Journal of Heat and Mass Transfer 2004;47:353–361.

[3] Shen SQ, Chen X, Mu XS, et al. Heat transfer characteristics of horizontal tube falling film evaporation for desalination. J. Desalination and Water Treatment 2014; 1–7.

[4] Nusselt. W, Die oberflachenkondensation des wasserdampfes, Zeitschr. Ver. Deut. Ing 1916;60(3): 541–575.

[5] Zhang Y-S, Wang DW, Liu Y. Distribution characteristics of falling film thickness around a horizontal corrugated tube. J. International Journal of Heat and Mass Transfer 2020;154:1-10.

[6] Hou H, Bi QC, Ma H. Distribution characteristics of falling film thickness around a horizontal tube. J. Desalination 2012;285:393–398

[7] Jayakumar A, Balachandran A, Mani A. Falling film thickness measurement using air-coupled ultrasonic transducer. J. Experimental Thermal and Fluid Science 2019; 109:1-9.

[8] Åkesjö A, Vamling L, Sasic S, et al. On the measuring of film thickness profiles and local heat transfer coefficients in falling films. J. Experimental Thermal and Fluid Science 2018;99:287–296.

[9] Han H, Wang SW, Li YX. 3–D Numerical study for the film thickness distribution of n–pentane falling film flow around the curved egg–shaped tube bundle. J. Chemical Engineering Research and Design 2020; 156:156–170

[10] Tahira F, Mabrouk A, Koç M. Impact of surface tension and viscosity on falling film thickness in multi-effect desalination (MED) horizontal tube evaporator. J. International Journal of Thermal Sciences 2020;150:1-14.

[11] Qiu QG , Meng CJ , Quan SL. 3-D simulation of flow behaviour and film distribution outside a horizontal tube. J. International Journal of Heat and Mass Transfer2017; 107:1028–1034.

[12] Wang J, Chen X, Lu T, et al. Three-dimensional film thickness distribution of horizontal tube falling film with column flow. J. Applied Thermal Engineering2019; 154 :140–149.

[13] Chen X, Shen SQ, Wang YX. Measurement on falling film thickness distribution around horizontal tube with laser-induced fluorescence technology J. International Journal of Heat and Mass Transfer2015;89:707–713.